Ovulatory Dysfunction and Compromised Granulosa Cells: Where does *Adar* fit?

By Rikki N. Nelson

Rikki Nicole Nelson
B.Sc., University of Wyoming, 2017

Submitted to the graduate degree program in Molecular and Integrative Physiology and the Graduate Faculty of the University of Kansas in partial fulfillment of the requirements for the degree of Master of Science.

_____
Committee Chair: Dr. Lane Christenson

_____
Dr. Michael Wolfe

_____
Dr. Gustavo Blanco

Date Defended: 10 July 2020

The thesis committee for Rikki N. Nelson certifies that this is the
approved version of the following thesis:

Ovulatory Dysfunction and Compromised Granulosa Cells: Where does *Adar* fit?

_____
Chair: Dr. Lane Christenson

_____
Graduate Director: Dr. Michael Wolfe

Date Approved: 15 July 2020

Abstract

Mural granulosa cells (mGCs) undergo waves of proliferation throughout the reproductive lifespan, and facilitate a timely gene expression response to the surge of luteinizing hormone in order to achieve ovulation and corpus luteum formation. High-throughput RNA sequencing has highlighted the amplitude of non-encoded RNA polymorphisms, particularly adenosine-to-inosine (A-to-I) transitions, in numerous tissues, but never in the somatic cells of the ovary. Such edits are catalyzed by the family of editing enzymes, adenosine deaminases acting on RNA (ADAR). Editing dependent and independent functions of adenosine deaminases acting on dsRNA affect codon usage, splice sites, transcript stability, and miRNA biogenesis. Physiological consequences of disrupting ADAR in murine cardiomyocytes and liver tissue include apoptosis and fibrosis. Utilizing *Adar*$^{FL/FL}$ /Aromatase$^{Cre/+}$ and wild-type control littermate female mice, the current thesis examines the role of *Adar* in mGCs. RNAScope was performed to confirm *Adar* depletion in mGCs. Fertility was assessed in a 7-month breeding trial, and morphology and state of fibrosis of the ovaries were evaluated using H&E and Picrosirius Red staining. Vaginal lavages were performed to confirm mating and visualize vaginal epithelium patterning. Ovulation was assessed via intraperitoneal injection of PMSG and hCG. Morphology of *Adar*$^{FL/FL}$ /Aromatase$^{Cre/+}$ ovaries at 16, 18, and 20 hours post-hCG administration was evaluated with H&E staining. Together, these data have shown that *Adar* in mGCs is critical for female fertility in mice. Mice lacking *Adar* exhibited extreme infertility with very few pups born despite recorded breeding attempts. Increased fibrosis was observed in ovaries of breeding trial mice lacking *Adar* compared to controls while H&E revealed intact follicles of varying sizes and the presence of luteal tissue. Estrous cycle pattern coordination was disrupted, and ovulation was delayed following exogenous gonadotropin administration. Oocytes were found trapped in follicles of a range of luteinization states in *Adar*$^{FL/FL}$ /Aromatase$^{Cre/+}$ ovaries. A lack of *Adar* in mGCs disrupts coordination of ovulation and luteinization, underscoring the fundamental role of *Adar* in granulosa cell physiology. Further studies to distinguish editing-dependent and editing-independent roles of ADAR in mGCs are warranted. Future investigations regarding the increased fibrosis observed in *Adar*$^{FL/FL}$ /Aromatase$^{Cre/+}$ breeding trial ovaries will determine the earliest age of significant fibrosis

accumulation in *Adar*$^{FL/FL}$/Aromatase$^{Cre/+}$ ovaries. Long term, studies may develop to evaluate the role of ADAR in balancing inflammation and immunity in mGCs to promote female fertility.

Acknowledgements

I would like to express a great appreciation for my advisor, Dr. Lane Christenson, for extending his mentorship over the course of my studies. His guidance continually fosters the spirit of scientific inquiry, scholarly adventure, and creative thought. All of which allowed this dissertation to be possible. I appreciate the space I was given to explore and communicate science in new ways. I would like to thank my lab-mates for only enhancing an encouraging environment.

I extend a thank you to my committee members for their guidance and leadership, and the Department of Molecular and Integrative Physiology, for upholding their mission to support students. Physiology Society has been irreplaceable in my success as a student of our department. Their championing of fellow students deserves great recognition.

I would also like to thank my friends and family, for without each and every one of you this would not have been possible. The Quad- Susan, Jacob, and Trae- is an undying source of stability and inspiration. I thank my partner, Don, for exemplifying compassion and steadiness, and helping me never lose sight of the purpose. Finally, I would like to thank my mother, Annette, your ability to distill positivity from any situation has lit my path. Your love and care have fueled the perseverance behind this achievement.

This work was funded by a grant from the Eunice Kennedy Shriver National Institute of Child Health & Human Development (NICHD). The grant number is HD094545 and is entitled Mitochondrial RNA defense pathways in the oocyte for the Principal Investigator, Lane Christenson. Additional funding sources include the Kathleen M. Osborn Fellowship in Reproductive Physiology 2017-2018. There are no conflicts of interest to report.

Table of Contents

List of Figures

Chapter 1: Introduction

Before the existence of the field of epitranscriptomics emerged, the phenomenon of RNA editing had been described (Benne et al. 1986). Since then, a paradigm developed to give structure to analyzing the observation of events in the transcriptome that are not reflected in the genome. Such observation encompasses methylation of a nucleotide to base modifications, termed RNA editing (Harcourt, Kietrys, and Kool 2017). More specifically, adenosine-to-inosine (A-to-I) editing was first observed in trypanosomes (Benne et al. 1986); then, it was found in a wide array of animals from flies (Palladino et al. 2000) to humans (U. Kim et al. 1994). The omnipresence of A-to-I editing across species spurred investigation into the causative factor, a family of enzymes called adenosine deaminases that act on dsRNA (ADARs) (Gerber and Keller 2001). ADARs and A-to-I editing have been described in a variety of murine tissues including brain, heart, liver, and testes (Melcher et al. 1996; El Azzouzi et al. 2020; Snyder, Licht, and Braun 2017; Ben-Shoshan et al. 2017). The body of knowledge surrounding *Adar* is comprised of tissue specific studies due to the embryonic lethal nature of an organism-wide *Adar* deletion in mice (Hartner et al. 2004). Therefore, the extent of the role of ADARs in female reproduction is largely unknown with published studies limited to the oocyte in *Xenapus laevis* and mice. (Saccomanno and Bass 1999; Brachova et al. 2019; García-López, Hourcade, and Del Mazo 2013). The function of ADARs in granulosa cells of the ovary has not been investigated prior to the thesis at present.

Variety is the splice of life with ADARs

In mice, the family of ADARs is composed of three enzymes. *Adar* (ADAR), *Adarb1* (ADAR2), and *Adarb2* (ADAR3). ADAR and ADAR2 are catalytically active, facilitating the signature A-to-I editing reaction while ADAR3 is not catalytically active but retains the ability to bind dsRNA (Chen et al. 2000). In A-to-I editing, the native adenosine base is deaminated, resulting in an inosine base. Inosines are interpreted as a guanosine (G) by the cellular machinery and sequencing technology, thus manifesting as an A-to-G mismatch in the RNA sequence to genomic sequence. ADAR2 is notorious for the critical editing event of glutamate receptor, ionotropic, AMPA2 (alpha 2; *Gria2*) receptor mRNA in the brain (Li and Church 2013). *Adarb1* null mice experience early onset seizures and die young. With the introduction

of a “G” in place of the native “A” in the alleles encoding the AMPA receptor in the *Adarb1* null background, the phenotype was rescued (Higuchi et al. 2000). Few site-specific editing events have been identified, mostly confined to brain tissue and attributed to ADAR2 (Sergeeva, Amberger, and Haas 2007). In contrast, *Adar* is more strongly expressed in the periphery (Eisenberg and Levanon 2018). *Adar* generates two isoforms; the smaller p110 is constitutively expressed and generally found in the nucleus, while the larger, cytoplasmic p150 is the interferon-inducible isoform (Patterson and Samuel 1995).
The mechanism by which ADARs recognize substrates is not well defined. A consensus sequence for binding domains of the ADARs has not been found. Substrate structure beyond the primary sequence is critical. The secondary structure of RNA is required for binding of ADAR and ADAR2, thus defining dsRNA binding domains, but ADAR3 binds ssRNA in addition to dsRNA (Chen et al. 2000). Further substrate specificity is influenced by the respective catalytic domains of ADAR and ADAR2 (Wong, Sato, and Lazinski 2001). Target specificity is strengthened by the necessity of ADAR2 for proper editing efficiency in the brain. Tertiary structure of dsRNA has been found to influence transcript editing site identification by positioning editing sites along a single side of the helix (Ensterö et al. 2009).
Mechanisms of initiation of target identification have remained elusive in mouse and human, but protein-protein interactions have been proposed in *Caenorhabditis elegans* (Rajendren et al. 2018). Additional *trans* regulators have been identified in flies (Sapiro et al. 2020) and human derived cell lines (Freund et al. 2020). RNA binding proteins containing domain associated with zinc fingers domains were found to regulate RNA editing by binding near editing sites, therefore competing for RNA binding (Freund et al. 2020). The pool of ADAR interacting proteins ranges from tissue-specific to editing-site-specific regulators. Such diversity emphasizes the wide range implications of ADAR physiology. Regardless of the complexities of target recognition, the consequences of ADAR functionality have been investigated. The canonical role of ADAR as an A-to-I editor has the immediate consequence of recoding individual bases; the lasting impact of recoding events range from altering codon usage, creating splice sites, changing miRNA targeting regions, altering miRNA sequences, and distinguishing endogenous RNA products from foreign molecules (Liddicoat et al. 2015). Chemically marking self RNA prevents

abnormal activation of innate immune system signaling meant to protect against viral infection (Mannion et al. 2014). In the presence of foreign dsRNA, mitochondrial antiviral signaling protein (MAVS) is activated by the dsRNA sensing protein melanoma differentiation-associated protein 5 (MDA5). Activated MAVS proteins aggregate, compromising mitochondrial integrity, and initiating mitochondrial-mediated inflammation (Sandhir, Halder, and Sunkaria 2017). Without the incorporation of inosine residues by ADAR, self dsRNA would activate the innate immune system, as occurs in Aicardi-Goutières Syndrome (AGS; Crow 2005). The interferon type I signature found in AGS patients is replicated in mice lacking catalytically active ADAR (Rice et al. 2012; Liddicoat, Chalk, and Walkley 2016). Prevention of aberrant innate immunity activation is apparent in murine erythropoiesis when compared to mice lacking *Adar* in erythroid cells (Liddicoat et al. 2016). A lack of mature erythroid cells is recapitulated with an erythroid-specific catalytically inactive *Adar* allele. Editing was detected in neighboring SINE elements on the wild-type background but was not detected in the absence of catalytically active ADAR, suggesting that regions of dsRNA were maintained. Together, their findings illustrate the physiological role of ADAR in erythroid cells as the canonical editing-dependent toleration of endogenous dsRNA (Liddicoat et al. 2016). While this study did not find significant differences in miRNA, others have displayed implications of ADAR in miRNA physiology.

ADAR-dependent effects have been identified in nuclear and cytoplasmic segments of miRNA biogenesis. Nuclear ADAR editing of pri-miRNA prevents loading and subsequent maturation processes facilitated by Drosha and DGCR8 (Yang et al. 2006). Hyperedited pri-miRNA is altogether removed from the miRNA maturation pathways by Tudor-SN mediated degradation (Yang et al. 2006; García-López, Hourcade, and Del Mazo 2013). While pre-miRNAs are edited in the cytoplasm, and editing at this step can prevent loading and further maturation by the Dicer complex (Iizasa et al. 2010; Kawahara, Zinshteyn, Chendrimada, et al. 2007). If editing does not halt the miRNA maturation process, the edited miRNA can be redirected to a new target mRNA (Pfeffer et al. 2005; Kawahara, Zinshteyn, Sethupathy, et al. 2007). Outside of the miRNA biogenesis, ADAR-mediated editing has been shown to alter miRNA

target sites of 3’ UTR thus rendering a transcript resistant to repression by miRNA or creating novel miRNA target sites (Liang and Landweber 2007; Tomaselli et al. 2013).

ADAR elicits additional effects on RNA metabolism. Human ADAR1 was shown to protect cytoplasmic transcripts by binding the 3’UTR and preventing Staufen-mediated mRNA decay in response to cellular stress (Sakurai et al. 2017). In the murine oocyte, ADAR-attributed inosines are enriched in the wobble position of codons and correlates with transcript stability during oocyte maturation (Brachova et al. 2019). It is proposed that the impact of altering transcript stability manifests as improper gene dosage in the mature egg, that then alters subsequent developmental processes. The physiological relevance in female reproduction outside of the oocyte has not been defined.

Mural Granulosa Cells

Ovulation is the ultimate product of the surge of luteinizing hormone (LH) produced by gonadotropes of the anterior pituitary gland. Mural granulosa cells (mGCs) of the preovulatory follicle coordinate the follicle with such ovulatory cues, as cumulus cells and the oocyte lack the cognate receptor, LHCGR. A multitude of effects of LHCGR activation have been compiled over the decades with three main themes culminating into granulosa cell terminal differentiation, oocyte maturation, and follicle rupture (Richards and Ascoli 2018). Mouse models are indispensable in these studies due to the ease of genetic manipulation and ability to exogenously control the estrous cycle through superovulation protocols of pregnant mare serum gonadotropin (PMSGG) administration followed by human chorionic gonadotropin (hCG) 48 hours later to mimic the endogenous LH surge. On average, ovulation is achieved approximately 11-14 hours after the surge in mice with several critical gene networks reaching the highest expression four hours post-hCG (Robker et al. 2000; J. Kim, Bagchi, and Bagchi 2009). However, gene expression changes can be detected as quickly as 1 hour post-hCG (Carletti and Christenson 2009). Attenuation of gene expression is as important as induction as illustrated in female mice lacking C/EBPβ. Without C/EBPβ, expression of *PTGS2* and Aromatase are not curtailed, resulting in infertility from a

failure to achieve ovulation (Sterneck, Tessarollo, and Johnson 1997). Fine tuning of a gene's expression and its product in mGCs is essential to adequately coordinate ovulation.

Not only do mGCs lay at the center of follicle survival to promote successful reproduction, mGCs also initiate follicular atresia. Apoptosis is first observed in the internal mGCs before spreading throughout the follicle ultimately resulting in whole follicle death (Da et al. 2012). The normal function of follicular atresia is to remove follicles that are not destined for ovulation. With age, the number of follicles subjected to atresia increases. This coincides with an increase of fibrosis within the ovarian stroma with age in mice (Briley et al. 2016). An increase in collagen deposition is observed in mice harboring genetic disruption of aromatase that exacerbates with age (Britt et al. 2000). It has been proposed that increased collagen and extracellular matrix deposition alters the stiffness of ovarian tissue and ultimately negatively affects the process of ovulation (Woodruff and Shea 2011). The explicit molecular mechanism behind the increase in ovarian fibrosis with age is unknown.

In general, post-transcriptional gene regulation enforces fine-tuning of gene expression without reprogramming at the nuclear level. Other tissues employ the ADARs to facilitate this fine-tuning through editing and non-editing dependent processes. *Adar* is the highest expressed adenosine deaminase in murine mural granulosa cells (Edgar, Domrachev, and Lash 2002; "NCBI GEO Database. Accession GSE80326" n.d.), yet there has been no insight into the physiological role of ADAR or the molecular mechanisms it enacts within mGCs. Here, the physiological consequences of mGC-specific *Adar* deletion are characterized. Granulosa cell competence was found to be compromised; an inadequate response to ovulatory cues was observed, resulting in female infertility. Utilizing this model, the editing effects of ADAR can be examined in preovulatory follicles since the gene is truncated during the gonadotropin dependent phase of growth. The deletion of *Adar* results in inflammation and fibrosis in the murine liver (Ben-Shoshan et al. 2017). While fibrosis occurs in the aged, wild-type murine ovary, the extent of fibrosis and collagen deposition observed in ovaries of 8-month-old mice lacking mGC *Adar* appears to be premature. *Adar* is necessary for normal granulosa cell physiology and maintaining female fertility.

Chapter 2: Granulosa cell specific loss of *Adar* delays ovulation, resulting in infertility in mice

Introduction

Studies in post-transcriptional gene regulation have revealed the ubiquity of mRNA modifications from deposition of chemical moieties as seen in *N*6-methyladenosine to complete catalysis of transition as seen in adenosine to inosine (A-to-I) editing (Harcourt, Kietrys, and Kool 2017). The factor deemed the "writer" of A-to-I editing is one family of enzymes, the adenosine deaminases acting on dsRNA (ADARs). Of the three members of this enzyme family, *Adar* (ADAR) and *Adarb1* (ADAR2) are catalytically active and facilitate the distinctive canonical editing function of ADAR enzymes, while *Adarb2* (ADAR3) does not catalyze the A-to-I transition (Brenda L. Bass 2002). All of the ADARs maintain the dsRNA binding domain, preserving the potential to elicit an effect through non-canonical mechanisms (Chen et al. 2000). This includes functional implications of ADARs in miRNA pathways from biogenesis to target recognition (Tomaselli et al. 2013; Kazuko Nishikura 2016), as well as in the ability to sequester transcripts from degradation (Sakurai et al. 2017). Effects of ADARs are ubiquitous, however *Adar* is often found to be more strongly expressed outside of the central nervous system (Eisenberg and Levanon 2018). *Adar* generates two isoforms; the smaller p110 is constitutively expressed and generally found in the nucleus, while the larger, cytoplasmic p150 is the interferon-inducible isoform (Patterson and Samuel 1995).

The widespread expression of *Adar*, and the status of A-to-I editing as the most prevalent mammalian RNA editing event (Picardi et al. 2015; Eisenberg and Levanon 2018; O'Connell 2015), begs the question of its physiological role. However, organism-wide *Adar* deletion is embryonic lethal due to liver disintegration and hematopoietic insufficiency in mice, preventing investigation in adult tissues (Hartner et al. 2004). Implementing models for spatially and temporally controlled *Adar* deletion has revealed a critical role in inducing organ fibrosis as a result of decreased cell proliferation and survival in the murine liver and the adult heart (Ben-Shoshan et al. 2017; El Azzouzi et al. 2020). A general function of ADAR has been proposed to protect against stress-induced apoptosis in developing vertebrae, heart, liver, and

mouse embryonic fibroblasts (Wang et al. 2004). These data indicate a need to explore the implications of loss of *Adar* in other proliferative tissues.

Periovulatory follicles provide an *in vivo* system to evaluate the consequences of *Adar* deletion. Mural granulosa cells (mGCs) of the ovarian follicle undergo cycles of proliferation and differentiation throughout each wave of follicle recruitment during the reproductive lifespan of an organism. Maintenance of mGC proliferation and differentiation in dominant follicles is fundamental to achieving ovulation and therefore female fertility (Richards and Ascoli 2018). The body of knowledge regarding mGC function allows for measurable outcomes of mGC manipulation. Utilizing the cohort of periovulatory follicles of the murine ovary, this study aims to characterize the phenotypic outcomes of *Adar* deletion in mGCs and assess the effects on female murine fertility.

Materials and Methods

Animals and Generation of Conditional Knockout

All procedures involving animals were reviewed and approved by the Institutional Animal Care and Use Committee at the University of Kansas Medical Center and were performed in accordance with the Guiding Principles for the Care and Use of Laboratory Animals. Such experiments were performed on conditional knockout female mice, $Adar^{FL/FL}$ /$Aromatase^{Cre/+}$, generated by breeding homozygous $Adar^{FL/FL}$ female mice with heterozygous $Aromatase^{Cre/+}$ and $Adar^{FL/FL}$ males. The $Adar^{FL/FL}$ mice were generously provided by Dr. Stuart H. Orkin (Harvard University), while the *Cyp19*-CRE mice were provided by Dr. Jan Gossen (Osteo-Pharma BV). The details of these mice are found in Hartner et al. 2004 and Fan et al. 2008. Briefly, under the granulosa cell-specific aromatase promoter, Cre-Recombinase excised lox-p sites flanking exons 7-9 of *Adar* resulting in a gene lacking the coding region corresponding to the deaminase domain. Mice were maintained in a humidity and temperature-controlled environment with a 14-h light, 10-h dark cycle (7 am to 9 pm) with ad libitum access to food and water.

Animal Experiments

Fertility was assessed by pairing female *Adar*$^{FL/FL}$/Aromatase$^{Cre/+}$ mice (42 days of age, n = 5) as well as wild-type control littermates (n=6) with adult wild-type C57BL/6J, 7-8-week-old males of known fertility. All females were continually exposed to males for 7 months. Female mice were euthanized at the conclusion of the breeding trial and ovaries were dissected away from the uterus proximal to the uterotubal junction, rinsed in sterile PBS and placed in cold 4% paraformaldehyde (PFA).

Vaginal cytology was characterized in sexually mature, 42-day old mice in absence of males and in those mice exposed to males during the breeding trial. Mice of 42 days of age were cycled for at least 21 days while *Adar*$^{FL/FL}$/Aromatase$^{Cre/+}$ females from the breeding trial were staged during the fifth month of the trial for 26 days. Wild-type control females from the breeding trial were not cycle staged due to pregnancy. All cycle staging was performed at 8:00-10:00 a.m. Approximately 200 µl of sterile saline was gently flushed into and aspirated from vaginal opening using a glass dropper. The aspirated lavage was then placed on glass slides and allowed to dry at room temperature. Smears were stained with 1% crystal violet in water (w/v) for 2 minutes, followed by gentle rinsing with water. Samples were mounted with 15 µl of glycerol and coverslip for microscopic visualization on a Nikon YS2-T microscope at 10X magnification.

Presence and relative abundance of leukocytes, nucleated epithelial cells, and cornified squamous epithelial cells was used to categorize mice into proestrus, estrus, metestrus, and diestrus (McLean et al. 2012). Presence of sperm, or visualization of a seminal plug preventing lavage in breeding trial females, was recorded as a positive mating.

Superovulation was induced in 21-day old mice via an intraperitoneal (i.p.) injection of 5 IU of pregnant mare serum gonadotropin (PMSG) (Calbiochem**)** followed by 5 IU of human chorionic gonadotropin (hCG) 46 hours after PMSG with relevant lengths of hCG (MilliporeSigma**)** exposure used for each experiment. To determine ovulation rates, mice were euthanized 16, 18, and 20 hours after hCG and ovaries and oviducts were collected by dissection distal to the uterotubal junction to ensure complete

removal of the oviduct without disruption. The oviduct and bursal encapsulated ovary were washed in dPBS before separation in warmed FHM media (MilliporeSigma) supplemented with bovine serum albumin (BSA) (4 mg/ml, MilliporeSigma) in 35 mm dishes. Cumulus oocyte complexes (COCs) were expressed from oviducts. COCs were transferred to 25 µl FHM media droplets containing 5 µl of hyaluronidase (MilliporeSigma) at 10 mg/mL for ten minutes to remove cumulus cells. Freed oocytes were counted and discarded.

RNAScope

RNAScope manual assay kit (Advanced Cell Diagnostics) was used following the manufacturer's protocol with modifications. Ovaries were collected from 6-week-old *Adar*$^{FL/FL}$ /Aromatase$^{Cre/+}$ (n=3) and wild-type littermates (n=3). Tissues were fixed in 4% PFA overnight at 4 °C before placement in 70% ethanol at 4 °C prior to paraffin embedding. Paraffin embedded ovarian tissues were sectioned at 7 µm and dried overnight. Slides were cleared of paraffin then hydrated in the recommended ethanol series. Endogenous peroxidases were quenched using the manufacturer's prepared H_2O_2 solution for ten minutes and washed in MilliQ water. Target retrieval was performed by suspending slides in gently boiling target retrieval solution for 15 minutes. Following MilliQ water washes and an ethanol wash, the slides were set at room temperature without humidity to allow a drawn hydrophobic barrier to dry. Protease inhibition was performed by incubation within a humidifying chamber. The chamber was assembled using a shallow tray with lid and humidifying paper. The tray was lined with parafilm along the rim to secure the lid. Slides were placed upon an aluminum foil strip on top of wet humidifying paper to allow for easy slide removal from the tray. The sealed tray was placed at 40 °C in a cell culture incubator with ambient air CO_2 and O_2 levels for 30 minutes. The *Adar* specific probe was designed to target bases 2212-2699, corresponding to the region of *Adar* that is deleted in conditional knockout females. The probe was hybridized to the target tissue for two hours within the humidifying chamber at 40 °C. Subsequent incubations for kit-labeled solutions AMP1-AMP4 were performed in the same tray and incubator, while kit-labeled AMP5-AMP6 were performed at room temperature within the tray, per protocol guidelines.

Slides were placed in prepared washing buffer in glass coplin jars with gentle agitation twice between each incubation. Approximately 100 µl of DAB substrate, which was modified from kit instructions based on the smaller tissue area (Advanced Cell Diagnostics), was utilized to detect the target signal. After the 10-minute incubation, slides were rinsed in MilliQ water. Counterstain was achieved by a two-minute incubation in hematoxylin droplets applied to tissue at room temperature with brief bluing by 1M ammonia water. After dehydration in the recommended ethanol series, slides were mounted and sealed with Cytoseal (ThermoFisher) and glass coverslip.

Histology

Ovaries collected for histological analysis were immediately placed in cold 4% paraformaldehyde. Fixation occurred overnight at 4 °C before ovaries were placed in 70% ethanol for paraffin embedding. Tissues were sectioned at 8 µm and stained with hematoxylin and eosin.

Additional 8 µm sections of ovarian tissue from breeding trial mice were stained with Picrosirius Red as previously described (Briley et al. 2016). Red intensity was quantified using the same protocol by quantifying red staining intensity on ImageJ (Briley et al. 2016; "Quantifying Stained Liver Tissue" n.d.)

Statistics

Statistical analysis was performed using GraphPad Prism (Version 8 GraphPad Software Inc. San Diego, CA). A *t*-test was performed to determine significance of PSR staining intensity and average litter size between groups. An ANOVA was used to determine the significance of the number of eggs retrieved from superovulation. P value < 0.05 was considered significant.

Results

Adar$^{FL/FL}$/Aromatase$^{Cre/+}$ mice show decreased detection of *Adar* via RNAScope while *Adar* was detected in wild-type littermate controls of the same age (Figure 1). *Adar*$^{FL/FL}$/Aromatase$^{Cre/+}$ female mice exhibit grievously diminished fertility, as shown by four of five *Adar*$^{FL/FL}$/Aromatase$^{Cre/+}$ mice failing to produce

offspring over a 7-month breeding trial. One *Adar*$^{FL/FL}$/Aromatase$^{Cre/+}$ female produced two small litters of four and five pups, while wild-type control female littermates (*Adar*$^{FL/FL}$ or $^{Fl/+}$, lacking Aromatase$^{Cre/+}$) all produced at least three litters each with an average of 8.0 ± 0.4 pups per litter (Figure 2). Normal breeding behaviors between breeding pairs was confirmed by visualization of a seminal plug or presence of sperm in vaginal smears of *Adar*$^{FL/FL}$/Aromatase$^{Cre/+}$ female mice. Plugs or sperm were found every 10-12 days (Figure 3). Cytology indicative of pseudopregnancy was observed in each smear between breeding events. Darkly stained leukocytes were seen in abundance with varying proportions of nucleated epithelial cells and few cornified epithelial cells (Figure 3). With positive breeding attempts recorded and appropriate pseudopregnancy evidence, *Adar*$^{FL/FL}$/Aromatase$^{Cre/+}$ fertility must be affected at the level of the internal reproductive tract.

At the conclusion of the breeding trial, female mice were euthanized to observe gross reproductive tract morphology. Uteruses appeared normal size in width and length as expected. Ovary sizes were not significantly different in *Adar*$^{FL/FL}$/Aromatase$^{Cre/+}$ specimens. Ovaries were collected for histological analysis due to Aromatase$^{Cre/+}$ expression confined to the gonad. Follicles of various sizes were seen in sections from the middle region of ovarian tissue in both *Adar*$^{FL/FL}$/Aromatase$^{Cre/+}$ and wild-type controls (Figure 4). Each display eosinophilic structures, indicating granulosa cell luteinization. Yellow to brown, multinucleated-cells were visualized in the stroma of each tissue. Picrosirius Red staining revealed an increase in extracellular matrix deposition, presumed to be collagen, in *Adar*$^{FL/FL}$/Aromatase$^{Cre/+}$ mid-region tissue sections when compared to breeding trial controls (Figure 5). Thus, disruption of *Adar* in granulosa cells impacts ovarian tissue composition in adult mice.

Estrous cycle staging was performed to determine if *Adar*$^{FL/FL}$/Aromatase$^{Cre/+}$ mice exhibited 4-5-day cycle patterns. Wild-type control mice progressed through cycle stages chronologically as expected, from proestrus, to estrus, to metestrus, through diestrus before repeating. However, *Adar*$^{FL/FL}$/Aromatase$^{Cre/+}$ mice did not exhibit any discernible cycle patterns, with prolonged periods of metestrus and diestrus observed. Proestrus was almost never identified (Figure 6). Disrupted estrous cycling indicates disrupted ovarian cycling, or an inability for the ovary to coordinate timely estrous patterning.

To determine if the disrupted cycling could be overcome, immature (21-day-old) mice were superovulated. Wild-type animals ovulated significantly more eggs (44.0 ± 8.0; n=11) than *Adar*$^{FL/FL}$/Aromatase$^{Cre/+}$ mice (0.75 ± 0.62; n=8). However, when oviduct dissection was postponed to 18 and 20 hours following hCG administration, more eggs were recovered (16.02 ± 8.06; n=5 and 7.3 ± 1.6; n=6, respectively) from *Adar*$^{FL/FL}$/Aromatase$^{Cre/+}$ mice (Figure 7). Eggs from wild-type control mice were released from oviducts as one large, cloud-like mass of multiple COCs while eggs from *Adar*$^{FL/FL}$/Aromatase$^{Cre/+}$ mice were extracted as individual COCs. As expected at 16 hours post-hCG, control ovaries displayed eosinophilic corpora lutea and evidence of follicle rupture (Figure 8). In *Adar*$^{FL/FL}$/Aromatase$^{Cre/+}$ ovaries, there were trapped oocytes often surrounded by densely compacted cumulus cells, and these follicles with trapped oocytes did not display evidence of luteinization at 16 hours post-hCG injection (Figure 8). However, trapped oocytes within luteinized follicles were observed in *Adar*$^{FL/FL}$ /Aromatase$^{Cre/+}$ ovaries at 18 hours post-hCG alongside antral follicles that had not yet been luteinized (Figure 8). Mixed populations of luteinized and not yet luteinized follicles were also observed at 20 hours post-hCG in *Adar*$^{FL/FL}$ /Aromatase$^{Cre/+}$ tissues. A delay in responding to gonadotropins results in dyssynchronous ovulation and luteinization, preventing the proper timing of fertilization and subsequent implantation.

Discussion

Granulosa cell specific knockdown of *Adar* guided by Aromatase-Cre recombinase activity produced female mice with severely diminished fertility. Despite observing positive breeding events, most *Adar*$^{FL/FL}$ /Aromatase$^{Cre/+}$ mice of the breeding trial failed to produce pups. Rhythmic estrous cycling was not observed in *Adar*$^{FL/FL}$ /Aromatase$^{Cre/+}$ mice, indicating a failure in ovarian controlled estrous patterning. While ovulation could be induced in *Adar*$^{FL/FL}$ /Aromatase$^{Cre/+}$ mice, the rate of ovulation was significantly decreased compared to wild-type controls. A modest increase in the number of eggs recovered from oviducts was observed with increased time between hCG administration and oviduct dissection. Differentiation of the ovarian somatic cells appeared to be sporadically delayed as well. At the conclusion

of the described breeding trial, increased macrophage presence and Picrosirius Red staining indicate an increase of fibrosis in *Adar*$^{FL/FL}$ /Aromatase$^{Cre/+}$ mice compared to wild-type littermate controls of the same age. These data suggest that mGCs of *Adar*$^{FL/FL}$ /Aromatase$^{Cre/+}$ ovaries are unable to coordinate differentiation into luteal cells and successful ovulation. Foundational studies utilizing a progesterone receptor deficient model report a complete obstruction of ovulation (Lydon et al. 1996), thus highlighting the critical role of mGC control and coordination in the periovulatory follicle. However, lack of progesterone receptor displayed a loss of mGC differentiation to luteal cells, while here we observed an inefficient mGC response to ovulatory, and succeeding, luteinization cues with eventual differentiation achieved.

In contrast to hormonal control of mGC function, the extent of inflammatory cues and inhibitions have also been defined. Inflammation mediated by *COX-2* is critical for ovulation to occur. *COX-2* $^{-/-}$ females are infertile due to defective ovulation and fertilization (Lim et al. 1997). The importance of timely expression of *COX-2* is highlighted with knockdown of the transcription factor CEBP/β. Without CEBP/β, the expression of *COX-2* is not attenuated, resulting in reduced ovulation in response to gonadotropins (Sterneck, Tessarollo, and Johnson 1997). The present study similarly describes a delay that does not result in absolute sterility, illustrated by the *Adar*$^{FL/FL}$/Aromatase$^{Cre/+}$ dam producing two smaller litters of pups and the recovery of a small number of eggs from the oviduct of superovulated *Adar*$^{FL/FL}$/Aromatase$^{Cre/+}$ mice, akin to what is seen in CEBP/β $^{-/-}$ mice. It is well documented that a lack of *Adar* induces inflammatory pathways in many tissues (Hartner et al. 2004; Pestal et al. 2015; Liddicoat, Chalk, and Walkley 2016; Bajad et al. 2020), but this has yet to be characterized in the ovary. The ovary is a unique tissue that requires a balance in inflammation for ovulation, and where imbalances in inflammation impact fertility.

Loss of *Adar* in other tissues has been shown to induce fibrosis in addition to inflammation (Ben-Shoshan et al. 2017). An increase in ovarian fibrosis and inflammation is observed with age (Briley et al. 2016). This correlates with the notion of decreased fertility with age in both humans and mice. A recent study displayed long term effects of manipulating the inflammasome within the ovary where an improved

reproductive rate at 12 months of age was observed by suppression of *NLRP3* (Navarro-Pando et al. 2020). Here we observed an increase in fibrosis of ovaries from *Adar*$^{FL/FL}$/Aromatase$^{Cre/+}$ mice compared to wild-type controls at eight months of age, suggesting a novel mechanism of inducing fibrosis in the ovary. An ongoing study is evaluating the role of loss of *Adar* induced inflammation and fibrosis in accelerated ovarian aging.

Implications of *Adar* deficiency have recently extended to miRNA biogenesis and processing (Yang et al. 2006; El Azzouzi et al. 2020). miRNA associated pathways are critical to female fertility from development (Hong et al. 2008) to modulating mature follicular atresia (Worku et al. 2017). Combined with our data, it is interesting to speculate the extent of the role of *Adar* in miRNA processing in mural granulosa cells.

Chapter 3: Additional Studies and Future Directions

Additional experiments have been designed with limited sample collection to supplement the studies reported in Chapter 2. While these additional experiments have not been carried out to completion, the training I had in aspects of design and specimen collection were instrumental to this thesis. Here, methodology used for collected samples and intended methods of analysis for such samples are described for transcriptomics and ovarian aging investigations in *Adar*$^{FL/FL}$ /Aromatase$^{Cre/+}$ mice and wild-type littermate controls.

Exploring A-to-I editing in granulosa cells

The study of epitranscriptomics has revealed over 50 RNA modifications in mammals (O'Connell 2015). These modifications range from methylation of nucleotides to catalytic conversion of one base to another (Harcourt, Kietrys, and Kool 2017). Knowledge of RNA modifications and the repercussions in the context of female reproduction is scant. Chemotherapy treatment was found to inhibit follicle development via an increase of N6-methyladenosine (m^6A) in granulosa cells (Huang et al. 2019). However, the changes in m^6A over the stages of folliculogenesis was not examined.

RNA A-to-I editing, a type of RNA modification, has recently been investigated in murine oocytes (Brachova et al. 2019). A-to-I editing is the conversion of adenosine to inosine by an adenosine deaminase acting on dsRNA (ADARs) (B. L. Bass and Weintraub 1988; Wagner et al. 1989; K. Nishikura et al. 1991). The A-to-I editing signature in oocytes was attributed to ADAR (*Adar*) and affected transcript stability during oocyte maturation (Brachova et al. 2019). ADAR is one of two catalytically active enzymes of the family of ADARs; ADAR2 (*Adarb1*) is also active, while ADAR3 (*Adarb2*) does not have catalytic activity (Melcher et al. 1996; Chen et al. 2000; Gerber and Keller 2001). Consequences of A-to-I editing manifest as changing codon usage, altering splice sites, changing miRNA targeting regions, altering miRNA sequences, and distinguishing endogenous RNA products from foreign molecules (Liddicoat, Chalk, and Walkley 2016; Eisenberg and Levanon 2018; Rueter, Dawson, and Emeson 1999; Tomaselli et al. 2013). Despite the widespread implications of A-to-I editing on post-transcriptional gene regulation and the status of *Adar* as the highest expressed adenosine deaminase in

granulosa cells ("NCBI GEO Database. Accession GSE80326" n.d.), it has not been studied in mural granulosa cells.

Mural granulosa cells exhibit acuity in gene expression in response to the LH surge in preparation for ovulation. Changes in gene expression are observed even one hour after the ovulatory cue (Carletti and Christenson 2009). Many genes identified as critical for ovulation peak in expression level approximately four hours after the cue (Robker et al. 2000; J. Kim, Bagchi, and Bagchi 2009). The significance of curtailing expression was observed in mice lacking C/EBPβ where prostaglandin expression was not attenuated, resulting in fettered ovulation (Sterneck, Tessarollo, and Johnson 1997). Mice with a granulosa cell specific deletion of *Adar* exhibit severely delayed or blocked ovulation resulting in infertility (Chapter 2). Due to A-to-I editing contributions to the precision of gene expression control, ADAR may elicit effects on granulosa cell physiology in an editing-dependent manner.

Materials and Methods

Granulosa Cell Collection

Adult 6-7-week-old *Adar*$^{FL/FL}$ /Aromatase$^{Cre/+}$ (see Chapter 2) and wild-type littermates were utilized for mural granulosa cell collection. Mice were hormonally stimulated with 5 IU of pregnant mare serum gonadotropin (PMSG; Calbiochem) via intraperitoneal injection (i.p.), followed 46 hours later with 5 IU of i.p. human chorionic gonadotropin (hCG; MilliporeSigma), and 4 hours after hCG administration mice were euthanized and ovaries were collected. Another group of *Adar*$^{FL/FL}$ /Aromatase$^{Cre/+}$ and wild-type littermates were subjected to 5 IU of PMSG for 46 hours and euthanized without hCG exposure. In summary, *Adar*$^{FL/FL}$ /Aromatase$^{Cre/+}$ at 46 hours of PMSG and 0 hours of hCG exposure (n=3), wild-type littermates at 46 hours of PMSG and 0 hours of hCG exposure (n=3), *Adar*$^{FL/FL}$ /Aromatase$^{Cre/+}$ at 46 hours of PMSG and 4 hours of hCG exposure (n=3), and wild-type littermates at 46 hours of PMSG and 4 hours of hCG exposure (n=3) have been collected and will be utilized, for a total of 4 experimental groups. Ovary and surrounding oviductal tissues were dissected at the uterotubal junction and away from the perigonadal fat pad. Ovaries were briefly washed in dPBS to remove blood and extra debris before

placement in FHM media (MilliporeSigma) supplemented with BSA (4 mg/ml, MilliporeSigma). The ovary was then carefully removed by cutting the bursa and peeling the membrane away from the tissue while being visualized under a Nikon SMZ1000 with Nikon NI-150 high intensity illuminator. All tissue beside the ovary was gently removed from the dish. Large follicles were visualized and punctured with 28-gauge needles to expel granulosa cells of preovulatory follicles. Punctured ovaries were removed from the dish and discarded. Individual oocytes and cumulus oocyte complexes were removed from the media using a mouth pipette. Suspended cells were transferred to 1.5 µl Eppendorf tubes and gently pelleted at 800 *g* at 4 °C for 7 minutes. Media was gently aspirated using a micropipette. 500 µl of TRI Reagent (Invitrogen) was applied to the cell pellet and RNA was isolated following the manufacturer's protocol.

RNA-Seq

RNA samples with quality values RIN > 8.0 as determined by Agilent TapeStation 4200 will be selected for direct RNA Nanopore sequencing. Approximately 500ng will be submitted for direct RNA sequencing using nanopore technology. Collected raw RNA-Seq data will be analyzed to detect gene expression differences between *Adar*$^{FL/FL}$ /Aromatase$^{Cre/+}$ and wild-type littermates both before hCG exposure and at 4 hours post hCG administration. Editing events will be detected and analyzed by comparing *Adar*$^{FL/FL}$ /Aromatase$^{Cre/+}$ to wild-type control littermates before and after hCG exposure.

For transcript abundance analysis, captured RNA-Seq data will undergo sequence alignment, and subsequently transcript abundance analysis. Methods previously established by our lab will be utilized (Brachova et al. 2019). Briefly, reads will be aligned against the mm10 *Mus musculus* curated database from RefSeq by Kallisto (Bray et al. 2016; O'Leary et al. 2016). Differential transcript abundance can then be determined between treatment groups using Sleuth (Pimentel et al. 2017).

For transcript editing analysis, RNA editing events again will be analyzed using methods previously used by our lab. The inosine bases will be identified using a pipeline composed of the Genome Analysis Tool Kit, (GATK), HiSAT2, Ensembl Variant Effect Predictor (VEP), and dbSNP (McLaren et al. 2016; D. Kim, Langmead, and Salzberg 2015; McKenna et al. 2010). HiSat2 and dbSNP will be used to align the sequence and disqualify single nucleotide polymorphisms as editing events. Then, RNA to DNA

differences are identified using GATK and HiSAT2. VEP is used to not only identify edited transcripts but classify where the edit occurs within the transcript and infer the consequence of the editing event on the transcript (DePristo et al. 2011; Ramaswami et al. 2013).

Expected Results

Expression of known LH induced genes is expected to b decreased in *Adar*$^{FL/FL}$ /Aromatase$^{Cre/+}$ at 4 hours post-hCG compared to wild-type controls at the same timepoint. Candidate genes include but are not limited to *CEBPB*, *Ptgs2*, *PGR*, *AREG*, *EREG*, *Btc*, and *3β-HSD*. It is expected that A-to-I editing will not occur, and therefore not be detected, in all *Adar*$^{FL/FL}$ /Aromatase$^{Cre/+}$ derived samples. It would be interesting to see if editing changes in the 3' UTR and has an effect on miRNA binding targets. Enrichment for inosine modifications at the wobble position may also be identified and further confirm the observation made in oocytes, colon, heart, large intestine, and stomach (Brachova et al. 2019).

Ovarian Aging

With age, the ovary becomes less efficient at follicle development and ovulation (Faddy 2000). This decrease coincides with increased granulosa cell death and overall decreased granulosa cell quality (Sadraie et al. 2000; Tatone and Amicarelli 2013). Stromal fibrosis has been shown to increase with age in mice (Briley et al. 2016). *Adar*$^{FL/FL}$ /Aromatase$^{Cre/+}$ female mice display a premature aging phenotype at 8 months of age when compared to wild-type littermates (Chapter 2). Loss of *Adar* has been shown to induce apoptosis and fibrosis in the liver and heart (Hartner et al. 2004; Ben-Shoshan et al. 2017; El Azzouzi et al. 2020). The contemporary trend of delaying childbearing until later in life has encouraged focus on mechanisms of ovarian aging in order to better understand and support such pregnancies. Utilizing a repository of aged murine tissues from *Adar*$^{FL/FL}$ /Aromatase$^{Cre/+}$ and wild-type littermates of ages 6 weeks, and 3, 6, 9, 12, and 16 months, the role of *Adar* in granulosa cells of aged ovaries will be investigated.

Materials and Methods

Animal Experiments

Adar$^{FL/FL}$/Aromatase$^{Cre/+}$ (generation previously described, this document) and wild-type littermates were utilized for mural granulosa cell collection. Female mice aged 6 weeks, 3, 6, 9, 12, and 16 months were administered 5 IU pregnant mare serum gonadotropin (PMSG) (Calbiochem) via intraperitoneal injection (i.p.), followed by 5 IU i.p. human chorionic gonadotropin (hCG) (MilliporeSigma) 46 hours later, and euthanization four hours following the last injection.

Ovary complexes were dissected at the uterotubal junction and perigonadal fat pad. One ovary, oviduct, and partial perigonadal fat pad were immediately placed in cold 4% paraformaldehyde (PFA) for fixation at 4 °C overnight before being placed in 70% ethanol for paraffin embedding. The other ovary was carefully removed from the bursal sac in dPBS under illumination of dissection scope (Nikon SMZ1000 with Nikon NI-150 high intensity illuminator) before being placed in FHM media (MilliporeSigma) supplemented with bovine serum albumin (BSA) (4 mg/ml, MilliporeSigma) in a 30mm plate on ice. Left and right perigonadal fat pads were dissected and evenly distributed to two Eppendorf tubes to determine fat weight before freezing in liquid nitrogen for storage at -80 °C for future use. Two 2-3mm uterine sections were dissected and frozen in liquid nitrogen for storage at -80 °C for future use. The ovary removed from the bursal sac was punctured with 28-gauge needles to expel follicular contents. Punctured ovaries were frozen in liquid nitrogen for storage at -80 °C for future use. Oocytes and cumulus oocyte complexes were removed from follicular contents via mouth pipette. Remaining cells, presumed to be mural granulosa cells in majority, were transferred to Eppendorf tubes. The remaining plate was placed on ice. Cells were gently pelletized at 800 *g* for 7 minutes and media was gently aspirated from the pellet. 500 µl of TRI Reagent (Invitrogen) was briefly applied to the plate kept on ice before immediately application to the cell pellet. The plate was briefly washed to collect all cells that stick to the plate. Aged ovaries that lacked follicular structures visualized under the dissecting scope were frozen in liquid nitrogen for storage at -80 °C for future homogenization for TRI Reagent application.

Histology

Ovary, oviduct, and perigonadal fat pad complexes PFA-fixed and paraffin embedded will be sectioned via microtome at 7-8 μm. Chronological sections will be stained with standard H&E and Picrosirius Red with Fast-Green, or Picrosirius Red alone, following protocols described by (Briley et al. 2016). Red staining intensity can be quantified on ImageJ using protocols previously described (Briley et al. 2016; "Quantifying Stained Liver Tissue" n.d.).

Expected Results

Adar$^{FL/FL}$ /Aromatase$^{Cre/+}$ mice display increased collagen deposition at 8 months of age compared to wild-type littermates of the same age (Chapter 2), so it is expected that *Adar*$^{FL/FL}$ /Aromatase$^{Cre/+}$ mice will display an increase of fibrosis at a younger age than wild-type counterparts. This would indicate that *Adar*$^{FL/FL}$ /Aromatase$^{Cre/+}$ exhibit premature ovarian aging, a phenotype associated with primary ovarian insufficiency in women. It would be interesting to evaluate the status of the NLRP3, caspase 1 and IL-1β in *Adar*$^{FL/FL}$ /Aromatase$^{Cre/+}$ mice, as these factors have been shown to be elevated in patients of primary ovarian insufficiency (Huhtaniemi et al. 2018). Attenuation of ovarian aging and prolonging of female fertility murine fertility was observed with inhibition of NLRP3-mediated inflammation (Navarro-Pando et al. 2020), so it is expected that *Adar* deletion would employ the reverse. If *Adar* expression decreases in granulosa cells with age, this could also contribute to the increase of fibrosis and inflammation with age.

Concluding Remarks

The ubiquitous expression and multitude of effects of ADARs has led to studies ranging from the brain to the liver (Melcher et al. 1996; Hartner et al. 2004; Ben-Shoshan et al. 2017). Now for the first time, the role of *Adar* in granulosa cell physiology has been investigated. *Adar* is necessary for murine female fertility, and without it, ovulation is severely delayed and the rate of ovulation is decreased. Granulosa cell luteinization is delayed in *Adar*$^{FL/FL}$ /Aromatase$^{Cre/+}$ mice, further contributing to an inadequate

response to the LH surge. An increase in ovarian fibrosis in *Adar*$^{FL/FL}$ /Aromatase$^{Cre/+}$ mice compared to wild-type littermates is observed at 8-months of age, indicative of a premature aging phenotype. It is interesting to speculate if the increased fibrosis, and therefore increased ovarian stiffness, contributes to a difficulty in follicular rupture necessary for ovulation as previously proposed (Woodruff and Shea 2011). The strong phenotypic characteristics of *Adar*$^{FL/FL}$ /Aromatase$^{Cre/+}$ female mice warrant further investigation into the molecular mechanisms behind these phenomena. Canonical functions of ADAR are manifestations of the signature A-to-I editing in altered codon usage, altered splice sites, edited miRNA binding sites, and edited miRNA seed sequences (Eisenberg and Levanon 2018). Each product can be investigated using the *Adar*$^{FL/FL}$ /Aromatase$^{Cre/+}$ model. Physiological consequences of *Adar*, or lack thereof, with age can be investigated using the repository of tissues collected for these studies. First, the progressive fibrosis can be characterized and the point of divergence of *Adar*$^{FL/FL}$ /Aromatase$^{Cre/+}$ mice from wild-type controls can be identified.

Creation and utilization of a novel mouse model will complement findings of *Adar*$^{FL/FL}$ /Aromatase$^{Cre/+}$ based studies. The initial model resulted in a truncated form of *Adar* upon aromatase expression from follicle stimulating hormone receptor activation, whereas the additional model will result in a modified product of *Adar* that is biotinylated by BirA ligase. Avi-tag-ADAR mice generated from breeding *Avi-Adar*, Aromatase$^{Cre/+}$, and BirA ligase genotype lines will produce an ADAR protein fused with a motif that can be biotinylated in granulosa cells by BirA ligase under Cre-recombinase control. By utilizing the biotinylation sequence, ADAR-containing complexes can be precipitated from cells via streptavidin recognition. Future studies would identify granulosa cell specific ADAR binding partners, and continue to develop our understanding of the role of ADAR in mural granulosa cells.

References

Bajad, Prajakta, Florian Ebner, Fabian Amman, Brigitta Szabó, Utkarsh Kapoor, Greeshma Manjali, Alwine Hildebrandt, Michael P. Janisiw, and Michael F. Jantsch. 2020. “An Internal Deletion of ADAR Rescued by MAVS Deficiency Leads to a Minute Phenotype.” *Nucleic Acids Research*, January. https://doi.org/10.1093/nar/gkaa025.

Bass, B. L., and H. Weintraub. 1988. “An Unwinding Activity That Covalently Modifies Its Double-Stranded RNA Substrate.” *Cell* 55 (6): 1089–98.

Bass, Brenda L. 2002. “RNA Editing by Adenosine Deaminases That Act on RNA.” *Annual Review of Biochemistry* 71: 817–46.

Benne, R., J. Van den Burg, J. P. Brakenhoff, P. Sloof, J. H. Van Boom, and M. C. Tromp. 1986. “Major Transcript of the Frameshifted coxII Gene from Trypanosome Mitochondria Contains Four Nucleotides That Are Not Encoded in the DNA.” *Cell* 46 (6): 819–26.

Ben-Shoshan, Shirley Oren, Polina Kagan, Maya Sultan, Zohar Barabash, Chen Dor, Jasmine Jacob-Hirsch, Alon Harmelin, et al. 2017. “ADAR1 Deletion Induces NFκB and Interferon Signaling Dependent Liver Inflammation and Fibrosis.” *RNA Biology* 14 (5): 587–602.

Brachova, Pavla, Nehemiah S. Alvarez, Xiaoman Hong, Sumedha Gunewardena, Kailey A. Vincent, Keith E. Latham, and Lane K. Christenson. 2019. “Inosine RNA Modifications Are Enriched at the Codon Wobble Position in Mouse Oocytes and Eggs.” *Biology of Reproduction*, July. https://doi.org/10.1093/biolre/ioz130.

Bray, Nicolas L., Harold Pimentel, Páll Melsted, and Lior Pachter. 2016. “Near-Optimal Probabilistic RNA-Seq Quantification.” *Nature Biotechnology* 34 (5): 525–27.

Briley, Shawn M., Susmita Jasti, Jennifer M. McCracken, Jessica E. Hornick, Barbara Fegley, Michele T. Pritchard, and Francesca E. Duncan. 2016. “Reproductive Age-Associated Fibrosis in the Stroma of the Mammalian Ovary.” *Reproduction* 152 (3): 245–60.

Britt, K. L., A. E. Drummond, V. A. Cox, M. Dyson, N. G. Wreford, M. E. Jones, E. R. Simpson, and J.

K. Findlay. 2000. “An Age-Related Ovarian Phenotype in Mice with Targeted Disruption of the Cyp 19 (aromatase) Gene.” *Endocrinology* 141 (7): 2614–23.

Carletti, Martha Z., and Lane K. Christenson. 2009. “Rapid Effects of LH on Gene Expression in the Mural Granulosa Cells of Mouse Periovulatory Follicles.” *Reproduction* 137 (5): 843–55.

Chen, C. X., D. S. Cho, Q. Wang, F. Lai, K. C. Carter, and K. Nishikura. 2000. “A Third Member of the RNA-Specific Adenosine Deaminase Gene Family, ADAR3, Contains Both Single- and Double-Stranded RNA Binding Domains.” *RNA* 6 (5): 755–67.

Crow, Yanick J. 2005. “Aicardi-Goutières Syndrome.” In *GeneReviews®*, edited by Margaret P. Adam, Holly H. Ardinger, Roberta A. Pagon, Stephanie E. Wallace, Lora J. H. Bean, Karen Stephens, and Anne Amemiya. Seattle (WA): University of Washington, Seattle.

Da1), Fuko Matsu, Naoko INOue2), Noboru MANAbe3), and Satoshi Ohku Ra1). 2012. “Follicular Growth and Atresia in Mammalian Ovaries: Regulation by Survival and Death of Granulosa Cells.” *The Journal of Reproduction and Development* 58 (1). https://www.jstage.jst.go.jp/article/jrd/58/1/58_2011-012/_pdf/-char/en.

DePristo, Mark A., Eric Banks, Ryan Poplin, Kiran V. Garimella, Jared R. Maguire, Christopher Hartl, Anthony A. Philippakis, et al. 2011. “A Framework for Variation Discovery and Genotyping Using next-Generation DNA Sequencing Data.” *Nature Genetics* 43 (5): 491–98.

Edgar, Ron, Michael Domrachev, and Alex E. Lash. 2002. “Gene Expression Omnibus: NCBI Gene Expression and Hybridization Array Data Repository.” *Nucleic Acids Research* 30 (1): 207–10.

Eisenberg, Eli, and Erez Y. Levanon. 2018. “A-to-I RNA Editing - Immune Protector and Transcriptome Diversifier.” *Nature Reviews. Genetics* 19 (8): 473–90.

El Azzouzi, Hamid, Andreia P. Vilaça, Dries A. M. Feyen, Willemijn M. Gommans, Roel A. de Weger, Pieter A. F. Doevendans, and Joost P. G. Sluijter. 2020. “Cardiomyocyte Specific Deletion of ADAR1 Causes Severe Cardiac Dysfunction and Increased Lethality.” *Frontiers in Cardiovascular Medicine* 7 (March): 30.

Ensterö, Mats, Chammiran Daniel, Helene Wahlstedt, François Major, and Marie Ohman. 2009.

"Recognition and Coupling of A-to-I Edited Sites Are Determined by the Tertiary Structure of the RNA." *Nucleic Acids Research* 37 (20): 6916–26.

Fan, Heng-Yu, Zhilin Liu, Nicola Cahill, and Joanne S. Richards. 2008. "Targeted Disruption of Pten Ovarian Granulosa Cells Enhances Ovulation and Extends the Life Span of Luteal Cells." *Molecular Endocrinology* 22 (9): 2128–40.

Faddy, M. J. 2000. "Follicle Dynamics during Ovarian Ageing." *Molecular and Cellular Endocrinology* 163 (1-2): 43–48.

Freund, Emily C., Anne L. Sapiro, Qin Li, Sandra Linder, James J. Moresco, John R. Yates 3rd, and Jin Billy Li. 2020. "Unbiased Identification of Trans Regulators of ADAR and A-to-I RNA Editing." *Cell Reports* 31 (7): 107656.

García-López, Jesús, Juan de Dios Hourcade, and Jesús Del Mazo. 2013. "Reprogramming of microRNAs by Adenosine-to-Inosine Editing and the Selective Elimination of Edited microRNA Precursors in Mouse Oocytes and Preimplantation Embryos." *Nucleic Acids Research* 41 (10): 5483–93.

Gerber, A. P., and W. Keller. 2001. "RNA Editing by Base Deamination: More Enzymes, More Targets, New Mysteries." *Trends in Biochemical Sciences* 26 (6): 376–84.

Harcourt, Emily M., Anna M. Kietrys, and Eric T. Kool. 2017. "Chemical and Structural Effects of Base Modifications in Messenger RNA." *Nature* 541 (7637): 339–46.

Hartner, Jochen C., Carolin Schmittwolf, Andreas Kispert, Albrecht M. Müller, Miyoko Higuchi, and Peter H. Seeburg. 2004. "Liver Disintegration in the Mouse Embryo Caused by Deficiency in the RNA-Editing Enzyme ADAR1." *The Journal of Biological Chemistry* 279 (6): 4894–4902.

Higuchi, M., S. Maas, F. N. Single, J. Hartner, A. Rozov, N. Burnashev, D. Feldmeyer, R. Sprengel, and P. H. Seeburg. 2000. "Point Mutation in an AMPA Receptor Gene Rescues Lethality in Mice Deficient in the RNA-Editing Enzyme ADAR2." *Nature* 406 (6791): 78–81.

Hong, Xiaoman, Lacey J. Luense, Lynda K. McGinnis, Warren B. Nothnick, and Lane K. Christenson. 2008. "Dicer1 Is Essential for Female Fertility and Normal Development of the Female

Reproductive System." *Endocrinology* 149 (12): 6207–12.

Huang, Boxian, Chenyue Ding, Qinyan Zou, Wei Wang, and Hong Li. 2019. "Cyclophosphamide Regulates N6-Methyladenosine and m6A RNA Enzyme Levels in Human Granulosa Cells and in Ovaries of a Premature Ovarian Aging Mouse Model." *Frontiers in Endocrinology* 10 (June): 415.

Huhtaniemi, Ilpo, Outi Hovatta, Antonio La Marca, Gabriel Livera, Danielle Monniaux, Luca Persani, Abdelkader Heddar, et al. 2018. "Advances in the Molecular Pathophysiology, Genetics, and Treatment of Primary Ovarian Insufficiency." *Trends in Endocrinology and Metabolism: TEM* 29 (6): 400–419.

Iizasa, Hisashi, Bjorn-Erik Wulff, Nageswara R. Alla, Manolis Maragkakis, Molly Megraw, Artemis Hatzigeorgiou, Dai Iwakiri, et al. 2010. "Editing of Epstein-Barr Virus-Encoded BART6 microRNAs Controls Their Dicer Targeting and Consequently Affects Viral Latency." *The Journal of Biological Chemistry* 285 (43): 33358–70.

Kawahara, Yukio, Boris Zinshteyn, Thimmaiah P. Chendrimada, Ramin Shiekhattar, and Kazuko Nishikura. 2007. "RNA Editing of the microRNA-151 Precursor Blocks Cleavage by the Dicer-TRBP Complex." *EMBO Reports* 8 (8): 763–69.

Kawahara, Yukio, Boris Zinshteyn, Praveen Sethupathy, Hisashi Iizasa, Artemis G. Hatzigeorgiou, and Kazuko Nishikura. 2007. "Redirection of Silencing Targets by Adenosine-to-Inosine Editing of miRNAs." *Science* 315 (5815): 1137–40.

Kim, Daehwan, Ben Langmead, and Steven L. Salzberg. 2015. "HISAT: A Fast Spliced Aligner with Low Memory Requirements." *Nature Methods* 12 (4): 357–60.

Kim, Jaeyeon, Indrani C. Bagchi, and Milan K. Bagchi. 2009. "Control of Ovulation in Mice by Progesterone Receptor-Regulated Gene Networks." *Molecular Human Reproduction* 15 (12): 821–28.

Kim, U., Y. Wang, T. Sanford, Y. Zeng, and K. Nishikura. 1994. "Molecular Cloning of cDNA for Double-Stranded RNA Adenosine Deaminase, a Candidate Enzyme for Nuclear RNA Editing." *Proceedings of the National Academy of Sciences of the United States of America* 91 (24): 11457–

61.

Li, Jin Billy, and George M. Church. 2013. “Deciphering the Functions and Regulation of Brain-Enriched A-to-I RNA Editing.” *Nature Neuroscience* 16 (11): 1518–22.

Liang, Han, and Laura F. Landweber. 2007. “Hypothesis: RNA Editing of microRNA Target Sites in Humans?” *RNA* 13 (4): 463–67.

Liddicoat, Brian J., Alistair M. Chalk, and Carl R. Walkley. 2016. “ADAR1, Inosine and the Immune Sensing System: Distinguishing Self from Non-Self.” *Wiley Interdisciplinary Reviews. RNA* 7 (2): 157–72.

Liddicoat, Brian J., Jochen C. Hartner, Robert Piskol, Gokul Ramaswami, Alistair M. Chalk, Paul D. Kingsley, Vijay G. Sankaran, et al. 2016. “Adenosine-to-Inosine RNA Editing by ADAR1 Is Essential for Normal Murine Erythropoiesis.” *Experimental Hematology* 44 (10): 947–63.

Liddicoat, Brian J., Robert Piskol, Alistair M. Chalk, Gokul Ramaswami, Miyoko Higuchi, Jochen C. Hartner, Jin Billy Li, Peter H. Seeburg, and Carl R. Walkley. 2015. “RNA Editing by ADAR1 Prevents MDA5 Sensing of Endogenous dsRNA as Nonself.” *Science* 349 (6252): 1115–20.

Lim, H., B. C. Paria, S. K. Das, J. E. Dinchuk, R. Langenbach, J. M. Trzaskos, and S. K. Dey. 1997. “Multiple Female Reproductive Failures in Cyclooxygenase 2-Deficient Mice.” *Cell* 91 (2): 197–208.

Lydon, John P., Francesco J. DeMayo, Orla M. Conneely, and Bert W. O’Malley. 1996. “Reproductive Phenotypes of the Progesterone Receptor Null Mutant Mouse.” *The Journal of Steroid Biochemistry and Molecular Biology* 56 (1): 67–77.

Mannion, Niamh M., Sam M. Greenwood, Robert Young, Sarah Cox, James Brindle, David Read, Christoffer Nellåker, et al. 2014. “The RNA-Editing Enzyme ADAR1 Controls Innate Immune Responses to RNA.” *Cell Reports* 9 (4): 1482–94.

McKenna, Aaron, Matthew Hanna, Eric Banks, Andrey Sivachenko, Kristian Cibulskis, Andrew Kernytsky, Kiran Garimella, et al. 2010. “The Genome Analysis Toolkit: A MapReduce Framework for Analyzing next-Generation DNA Sequencing Data.” *Genome Research* 20 (9): 1297–1303.

McLaren, William, Laurent Gil, Sarah E. Hunt, Harpreet Singh Riat, Graham R. S. Ritchie, Anja Thormann, Paul Flicek, and Fiona Cunningham. 2016. “The Ensembl Variant Effect Predictor.” *Genome Biology* 17 (1): 122.

McLean, Ashleigh C., Nicolas Valenzuela, Stephen Fai, and Steffany A. L. Bennett. 2012. “Performing Vaginal Lavage, Crystal Violet Staining, and Vaginal Cytological Evaluation for Mouse Estrous Cycle Staging Identification.” *Journal of Visualized Experiments: JoVE*, no. 67 (September): e4389.

Melcher, T., S. Maas, A. Herb, R. Sprengel, M. Higuchi, and P. H. Seeburg. 1996. “RED2, a Brain-Specific Member of the RNA-Specific Adenosine Deaminase Family.” *The Journal of Biological Chemistry* 271 (50): 31795–98.

Navarro-Pando, José M., Elísabet Alcocer-Gómez, Beatriz Castejón-Vega, Jordi Muntané, Pedro Bullon, Chun Wang, Hal M. Hoffman, et al. 2020. “Inhibition of the NLRP3 Inflammasome Prevents Ovarian Aging.” *bioRxiv*. https://doi.org/10.1101/2020.04.26.062646.

“NCBI GEO Database. Accession GSE80326.” n.d. Accessed May 28, 2020. https://www.ncbi.nlm.nih.gov/geo/query/acc.cgi?acc=GSE80326.

Nishikura, Kazuko. 2016. “A-to-I Editing of Coding and Non-Coding RNAs by ADARs.” *Nature Reviews. Molecular Cell Biology* 17 (2): 83–96.

Nishikura, K., C. Yoo, U. Kim, J. M. Murray, P. A. Estes, F. E. Cash, and S. A. Liebhaber. 1991. “Substrate Specificity of the dsRNA Unwinding/modifying Activity.” *The EMBO Journal* 10 (11): 3523–32.

O’Connell, Mary. 2015. “RNA Modification and the Epitranscriptome; the next Frontier.” *RNA* 21 (4): 703–4.

O’Leary, Nuala A., Mathew W. Wright, J. Rodney Brister, Stacy Ciufo, Diana Haddad, Rich McVeigh, Bhanu Rajput, et al. 2016. “Reference Sequence (RefSeq) Database at NCBI: Current Status, Taxonomic Expansion, and Functional Annotation.” *Nucleic Acids Research* 44 (D1): D733–45.

Palladino, M. J., L. P. Keegan, M. A. O’Connell, and R. A. Reenan. 2000. “dADAR, a Drosophila Double-Stranded RNA-Specific Adenosine Deaminase Is Highly Developmentally Regulated and Is

Itself a Target for RNA Editing." *RNA* 6 (7): 1004–18.

Patterson, J. B., and C. E. Samuel. 1995. "Expression and Regulation by Interferon of a Double-Stranded-RNA-Specific Adenosine Deaminase from Human Cells: Evidence for Two Forms of the Deaminase." *Molecular and Cellular Biology* 15 (10): 5376–88.

Pestal, Kathleen, Cory C. Funk, Jessica M. Snyder, Nathan D. Price, Piper M. Treuting, and Daniel B. Stetson. 2015. "Isoforms of RNA-Editing Enzyme ADAR1 Independently Control Nucleic Acid Sensor MDA5-Driven Autoimmunity and Multi-Organ Development." *Immunity* 43 (5): 933–44.

Pfeffer, Sébastien, Alain Sewer, Mariana Lagos-Quintana, Robert Sheridan, Chris Sander, Friedrich A. Grässer, Linda F. van Dyk, et al. 2005. "Identification of microRNAs of the Herpesvirus Family." *Nature Methods* 2 (4): 269–76.

Picardi, Ernesto, Caterina Manzari, Francesca Mastropasqua, Italia Aiello, Anna Maria D'Erchia, and Graziano Pesole. 2015. "Profiling RNA Editing in Human Tissues: Towards the Inosinome Atlas." *Scientific Reports* 5 (October): 14941.

Pimentel, Harold, Nicolas L. Bray, Suzette Puente, Páll Melsted, and Lior Pachter. 2017. "Differential Analysis of RNA-Seq Incorporating Quantification Uncertainty." *Nature Methods* 14 (7): 687–90.

"Quantifying Stained Liver Tissue." n.d. Accessed May 29, 2020. https://imagej.nih.gov/ij/docs/examples/stained-sections/index.html.

Rajendren, Suba, Aidan C. Manning, Haider Al-Awadi, Kentaro Yamada, Yuichiro Takagi, and Heather A. Hundley. 2018. "A Protein-Protein Interaction Underlies the Molecular Basis for Substrate Recognition by an Adenosine-to-Inosine RNA-Editing Enzyme." *Nucleic Acids Research* 46 (18): 9647–59.

Ramaswami, Gokul, Rui Zhang, Robert Piskol, Liam P. Keegan, Patricia Deng, Mary A. O'Connell, and Jin Billy Li. 2013. "Identifying RNA Editing Sites Using RNA Sequencing Data Alone." *Nature Methods* 10 (2): 128–32.

Rice, Gillian I., Paul R. Kasher, Gabriella M. A. Forte, Niamh M. Mannion, Sam M. Greenwood, Marcin Szynkiewicz, Jonathan E. Dickerson, et al. 2012. "Mutations in ADAR1 Cause Aicardi-Goutières

Syndrome Associated with a Type I Interferon Signature." *Nature Genetics* 44 (11): 1243–48.

Richards, Joanne S., and Mario Ascoli. 2018. "Endocrine, Paracrine, and Autocrine Signaling Pathways That Regulate Ovulation." *Trends in Endocrinology and Metabolism: TEM* 29 (5): 313–25.

Robker, R. L., D. L. Russell, L. L. Espey, J. P. Lydon, B. W. O'Malley, and J. S. Richards. 2000. "Progesterone-Regulated Genes in the Ovulation Process: ADAMTS-1 and Cathepsin L Proteases." *Proceedings of the National Academy of Sciences of the United States of America* 97 (9): 4689–94.

Rueter, S. M., T. R. Dawson, and R. B. Emeson. 1999. "Regulation of Alternative Splicing by RNA Editing." *Nature* 399 (6731): 75–80.

Saccomanno, L., and B. L. Bass. 1999. "A Minor Fraction of Basic Fibroblast Growth Factor mRNA Is Deaminated in Xenopus Stage VI and Matured Oocytes." *RNA* 5 (1): 39–48.

Sadraie, S. H., H. Saito, T. Kaneko, T. Saito, and M. Hiroi. 2000. "Effects of Aging on Ovarian Fecundity in Terms of the Incidence of Apoptotic Granulosa Cells." *Journal of Assisted Reproduction and Genetics* 17 (3): 168–73.

Sakurai, Masayuki, Yusuke Shiromoto, Hiromitsu Ota, Chunzi Song, Andrew V. Kossenkov, Jayamanna Wickramasinghe, Louise C. Showe, et al. 2017. "ADAR1 Controls Apoptosis of Stressed Cells by Inhibiting Staufen1-Mediated mRNA Decay." *Nature Structural & Molecular Biology* 24 (6): 534–43.

Sandhir, Rajat, Avishek Halder, and Aditya Sunkaria. 2017. "Mitochondria as a Centrally Positioned Hub in the Innate Immune Response." *Biochimica et Biophysica Acta, Molecular Basis of Disease* 1863 (5): 1090–97.

Sapiro, Anne L., Emily C. Freund, Lucas Restrepo, Huan-Huan Qiao, Amruta Bhate, Qin Li, Jian-Quan Ni, Timothy J. Mosca, and Jin Billy Li. 2020. "Zinc Finger RNA-Binding Protein Zn72D Regulates ADAR-Mediated RNA Editing in Neurons." *Cell Reports* 31 (7): 107654.

Sergeeva, Olga A., Bettina T. Amberger, and Helmut L. Haas. 2007. "Editing of AMPA and Serotonin 2C Receptors in Individual Central Neurons, Controlling Wakefulness." *Cellular and Molecular Neurobiology* 27 (5): 669–80.

Snyder, Elizabeth M., Konstantin Licht, and Robert E. Braun. 2017. “Testicular Adenosine to Inosine RNA Editing in the Mouse Is Mediated by ADARB1.” *Biology of Reproduction* 96 (1): 244–53.

Sterneck, E., L. Tessarollo, and P. F. Johnson. 1997. “An Essential Role for C/EBPbeta in Female Reproduction.” *Genes & Development* 11 (17): 2153–62.

Tatone, Carla, and Fernanda Amicarelli. 2013. “The Aging Ovary—the Poor Granulosa Cells.” *Fertility and Sterility* 99 (1): 12–17.

Tomaselli, Sara, Barbara Bonamassa, Anna Alisi, Valerio Nobili, Franco Locatelli, and Angela Gallo. 2013. “ADAR Enzyme and miRNA Story: A Nucleotide That Can Make the Difference.” *International Journal of Molecular Sciences* 14 (11): 22796–816.

Wagner, R. W., J. E. Smith, B. S. Cooperman, and K. Nishikura. 1989. “A Double-Stranded RNA Unwinding Activity Introduces Structural Alterations by Means of Adenosine to Inosine Conversions in Mammalian Cells and Xenopus Eggs.” *Proceedings of the National Academy of Sciences of the United States of America* 86 (8): 2647–51.

Wang, Qingde, Mana Miyakoda, Weidong Yang, Jaspal Khillan, David L. Stachura, Mitchell J. Weiss, and Kazuko Nishikura. 2004. “Stress-Induced Apoptosis Associated with Null Mutation of ADAR1 RNA Editing Deaminase Gene.” *The Journal of Biological Chemistry* 279 (6): 4952–61.

Wong, S. K., S. Sato, and D. W. Lazinski. 2001. “Substrate Recognition by ADAR1 and ADAR2.” *RNA* 7 (6): 846–58.

Woodruff, Teresa K., and Lonnie D. Shea. 2011. “A New Hypothesis Regarding Ovarian Follicle Development: Ovarian Rigidity as a Regulator of Selection and Health.” *Journal of Assisted Reproduction and Genetics* 28 (1): 3–6.

Worku, Tesfaye, Zia Ur Rehman, Hira Sajjad Talpur, Dinesh Bhattarai, Farman Ullah, Ngabu Malobi, Tesfaye Kebede, and Liguo Yang. 2017. “MicroRNAs: New Insight in Modulating Follicular Atresia: A Review.” *International Journal of Molecular Sciences* 18 (2). https://doi.org/10.3390/ijms18020333.

Yang, Weidong, Thimmaiah P. Chendrimada, Qingde Wang, Miyoko Higuchi, Peter H. Seeburg, Ramin

Shiekhattar, and Kazuko Nishikura. 2006. “Modulation of microRNA Processing and Expression through RNA Editing by ADAR Deaminases.” *Nature Structural & Molecular Biology* 13 (1): 13–21.

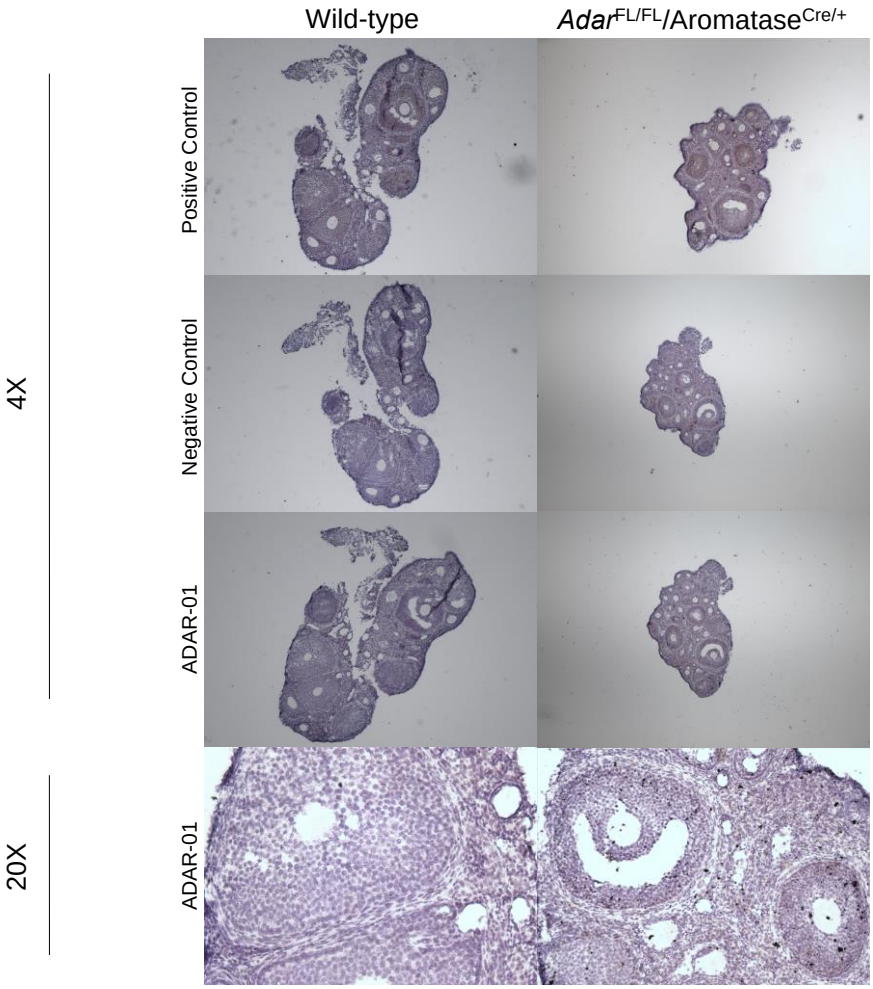

Figure 1. Preliminary RNAScope observations display successful completion of the technique on ovarian tissue using kit provided positive and negative control probes on *Adar*$^{FL/FL}$ /Aromatase$^{Cre/+}$ (n=3) and wild-type littermate controls (n=3). Detection of *Adar* is seen in granulosa cells of wild-type samples as brown speckles that are not seen in *Adar*$^{FL/FL}$ /Aromatase$^{Cre/+}$ derived samples.

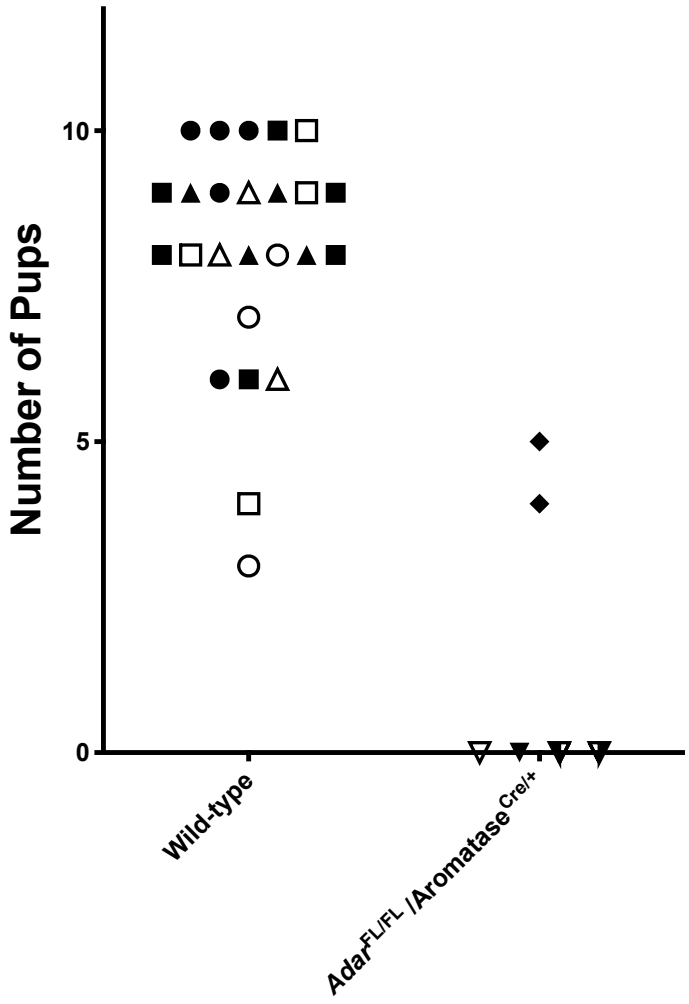

Figure 2. Breeding trial litter counts. Pups per litter for *Adar*$^{FL/FL}$ /Aromatase$^{Cre/+}$ (n= 5) and wild-type littermate control mice (n= 6) were counted over a 7-month period. Individual mice are indicated by unique icons. Each litter is plotted by the number of pups counted or placed at zero to indicate no litters were ever observed. Control mice had an average of 8.0 ± 0.4 pups/litter.

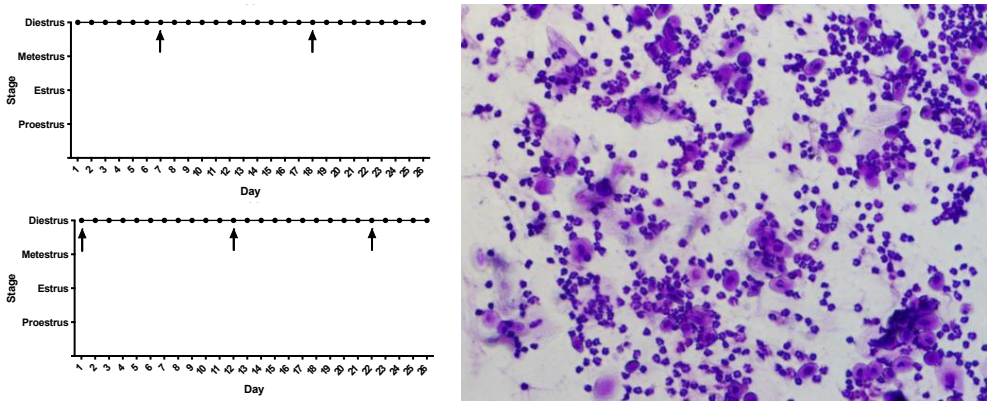

Figure 3. Vaginal cytology *Adar*$^{FL/FL}$ /Aromatase$^{Cre/+}$ breeding trial mice. Smears displayed an abundance of leukocytes characteristic of pseudopregnancy. Representative image of daily observed cytology is shown. Breeding events are indicated with black arrows. A seminal plug or sperm in the smear was visualized at regular intervals, approximately every 10 days.

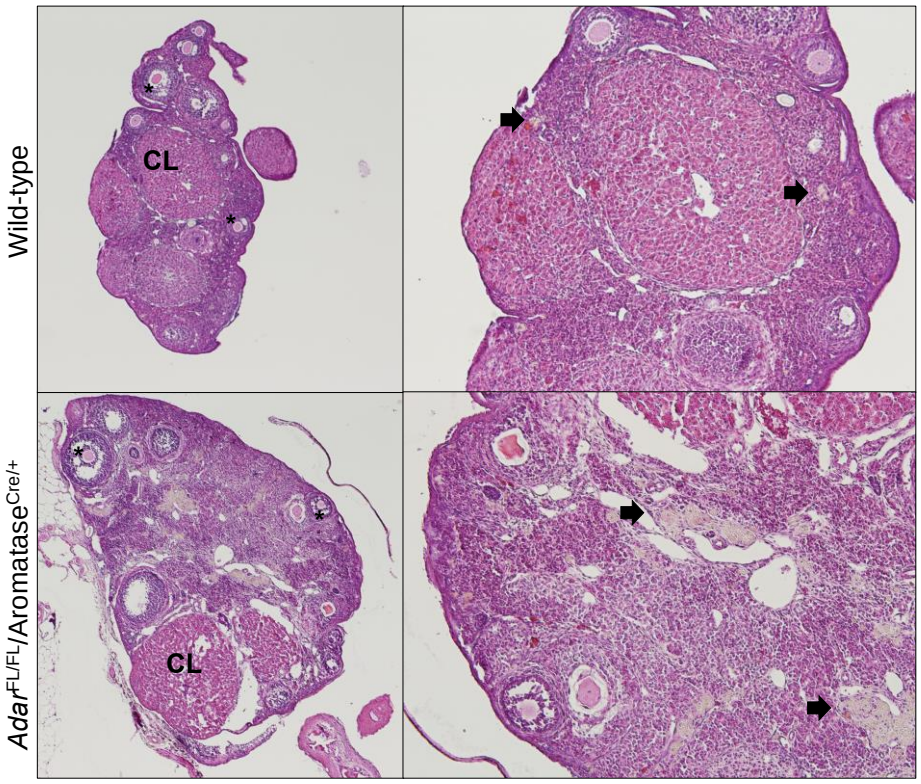

Figure 4. Histology of ovaries from *Adar*$^{FL/FL}$ /Aromatase$^{Cre/+}$ (n= 5) and wild-type littermate control breeding trial mice (n= 6). Sections from the middle region of tissue were selected for H&E staining. Control ovaries display corpora lutea (CL) and follicles (asterisk *) of varying size. Ovaries from conditional knockout females display fewer corpora lutea and similar follicle sizes. Yellow-multinucleated (arrows) cells can be seen in all ovaries with an increase in average in conditional knockout ovaries.

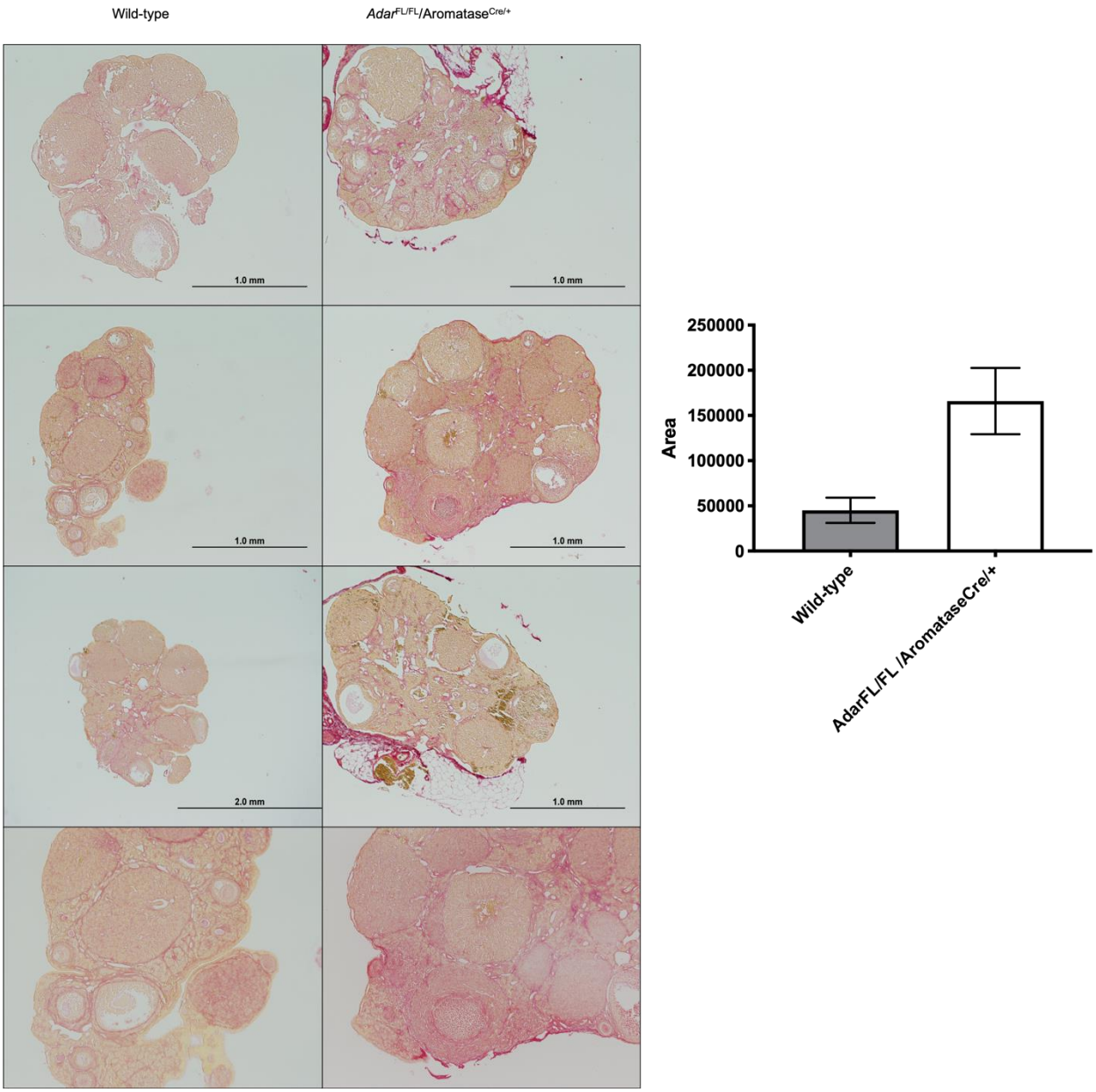

Figure 5. Picrosirius Red Staining was calculated using the area of the tissue of interest, excluding all tissues outside of the body of the ovary. Wild-type mice have red staining intensity of 45133 ± 14019 pixels/μm^2 (n=3) while *Adar*$^{FL/FL}$ /Aromatase$^{Cre/+}$ mice have increased intensity at 166005 ± 36643 pixels/μm^2 (n=4; p=0.04). Bottom panels provide higher magnification of tissues featured above.

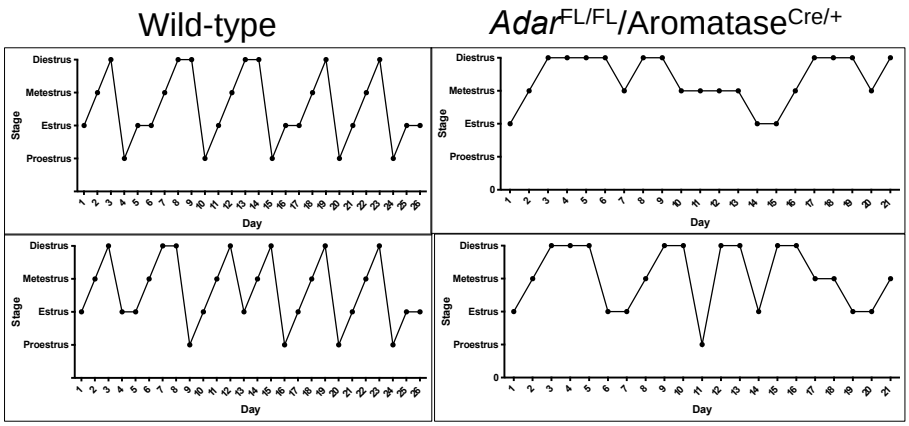

Figure 6. Estrous cycle stage was determined for *Adar*$^{FL/FL}$ /Aromatase$^{Cre/+}$ (n= 3) and wild-type females (n= 3). Vaginal smears were collected from 42-day old female mice for at least 21 days. Smears were staged as based upon cytology visualized by crystal violet staining. Representative graphs of chronological stages observed for each genotype are shown. *Adar*$^{FL/FL}$ /Aromatase$^{Cre/+}$ have disrupted cycling with prolonged periods of diestrus and metestrus while wild-type controls display the expected cyclical pattern.

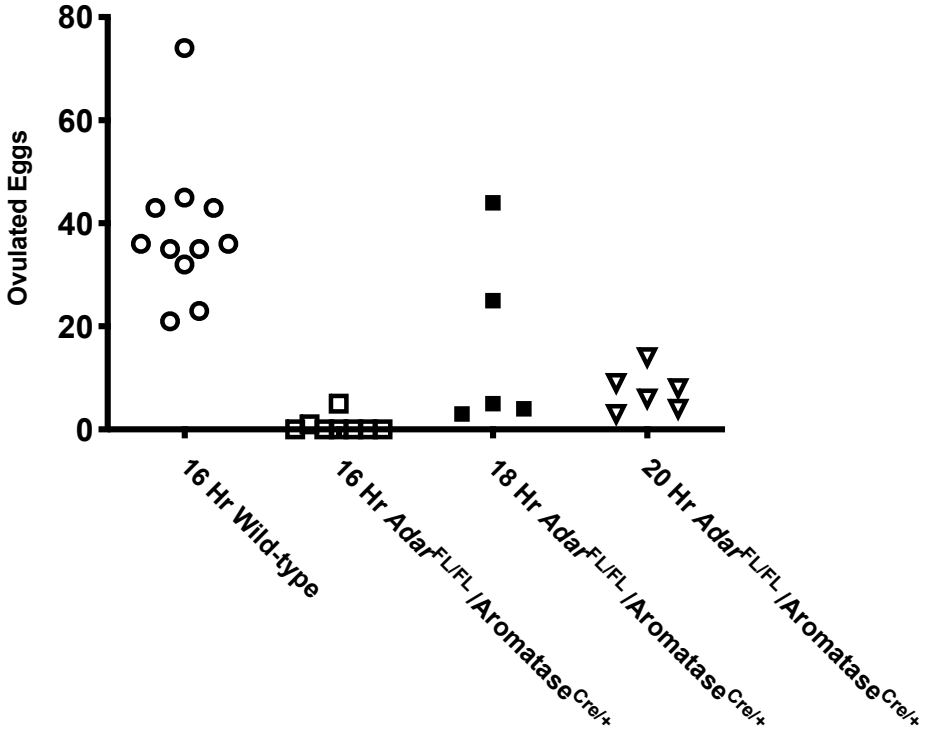

Figure 7. Ovulated eggs retrieved from oviducts 16, 18, and 20 hours after ovulation induction. Eggs were collected from oviducts of immature, 24-day-old wild-type and *Adar*$^{FL/FL}$ /Aromatase$^{Cre/+}$ after 46 hours of PMSG stimulation followed by 16 hours (44.0 ± 8.0; n=11) or 16 hours (0.75 ± 0.62; n= 8), 18 hours (16.02 ± 8.06; n= 5), and 20 hours (7.3 ± 1.6; n= 6) of hCG treatment, respectively. *Adar*$^{FL/FL}$ /Aromatase$^{Cre/+}$ mice exhibit a delay and reduction in the number of eggs ovulated compared to wild-type controls.

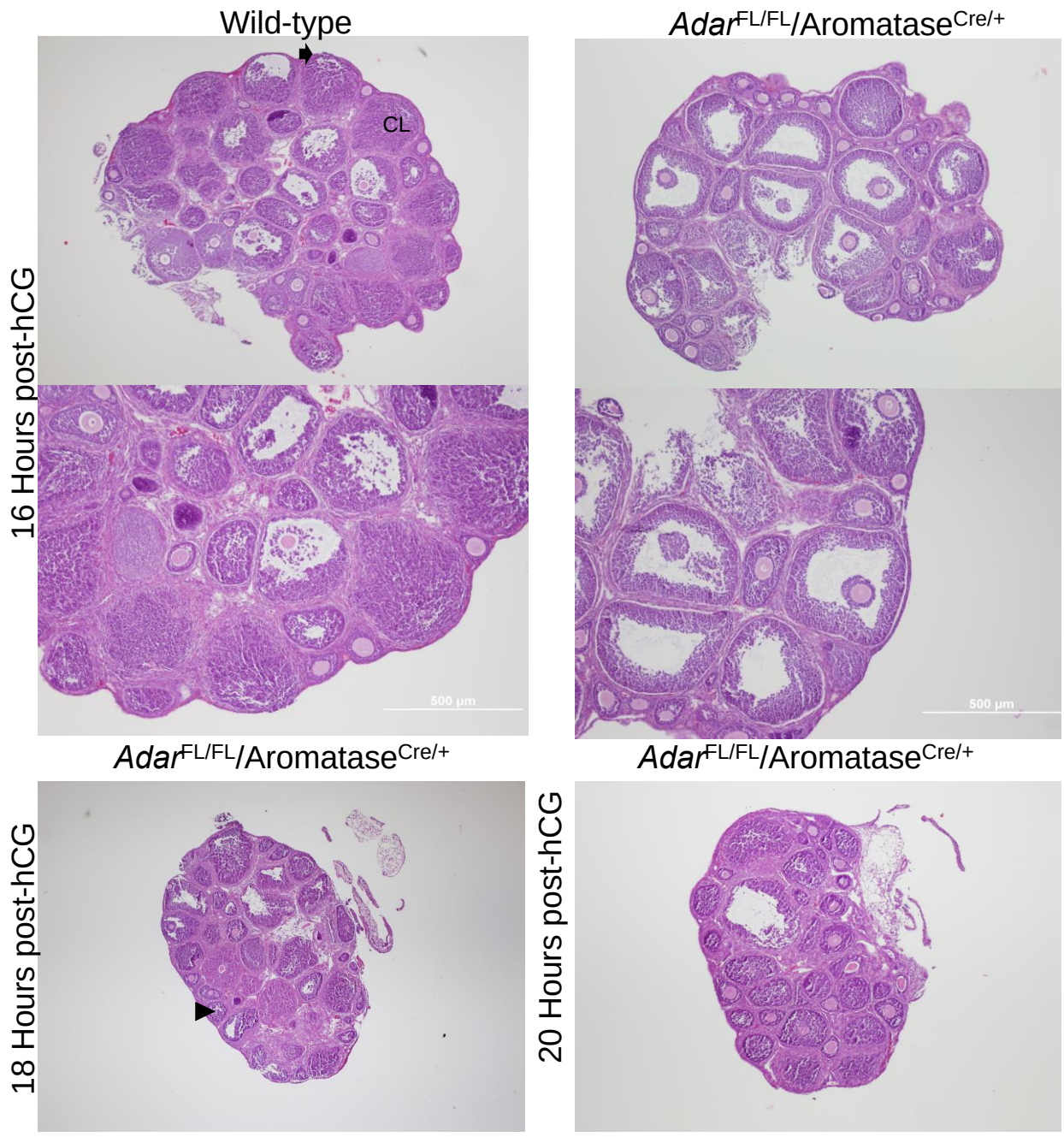

Figure 8. Histology of ovaries from immature superovulated wild-type and *Adar*$^{FL/FL}$ /Aromatase$^{Cre/+}$ mice. H&E staining of wild-type ovaries display corpora lutea (CL) and ovulation sites (arrow) while *Adar*$^{FL/FL}$ /Aromatase$^{Cre/+}$ ovaries display trapped oocytes with lack of luteinization of follicles at 16 hours post-hCG administration. Variation in luteinized follicles with trapped oocytes (arrowhead) are observed at 18 and 20 hours post-hCG administration.